COMPOSITION OF THE IIIF IRONS AND THEIR RELATIONSHIP TO THE ZINDER PALLASITE. M. Humayun[1], J. S. Boesenberg[2] and D. Van Niekerk[3] [1]National High Magnetic Field Laboratory, and Dept. of Earth, Ocean & Atmospheric Science, Florida State University, Tallahassee, FL 32310, USA (humayun@magnet.fsu.edu); [2]Dept of Earth, Environmental and Planetary Sciences, Brown University, Providence, RI 02920, USA; [3]Dept of Geology, Rhodes University, P.O. Box 94, Grahamstown 6140, South Africa.

Introduction: Magmatic iron meteorites, characterized by large ranges in their Ir abundances, represent the cores of numerous differentiated asteroidal bodies. Relating such irons to their silicate equivalents is not easy, except in cases where silicates are present in the irons: IIE, IVAs, etc., where O, Cr, Ti,etc., isotopes isotopes provide crucial links between irons and achondrites [1,2]. Recent work reveals the presence of two distinct trends of nucleosynthetic Mo isotopes in chondrites, with C chondrites (CC) plotting on a distinct trend from the Earth, ordinary, enstatite, and other chondrites, argued to be a trend for non-carbonaceous (NC) chondritic objects [3,4]. Many magmatic iron meteorites plot along the NC line in Mo isotopes, but some groups of magmatic irons (IIC, IID, IIF, IIIF, IVB) follow the CC line. These irons have been interpreted to originate by differentiation of carbonaceous chondrite parent bodies possibly in orbits beyond Jupiter [4]. The link between magmatic irons plotting on the CC line and material with CC-like isotopic composition in lithophile elements, including O, could be tested if silicate-bearing members of these groups were identified. Boesenberg et al. [5] reported that the metal of the pyroxene pallasite, Zinder, exhibited chemical similarities to the IIIF irons, which would make it the first silicate-bearing CC-iron. One limitation encountered by [5] was that the siderophile element data for the IIIF irons was relatively sparse. In this study, we report new siderophile element data collected on Zinder metal, and six of the eight known IIIF irons described, by LA-ICP-MS. We also analyzed Fitzwater Pass, classified as a possible IIIF.

Samples and Analytical methods: The irons Clark County, Klamath Falls, Moonbi, Nelson County, Oakley and Saint Genevieve County were obtained as polished slabs from USNM. A polished slab of Klamath Falls was obtained from AMNH. The same slab of Zinder analyzed by [5] was reanalyzed in this study to provide precise Ge abundances. LA-ICP-MS analyses were performed on an ElectroScientific Instruments New Wave™ UP193FX laser system coupled to a Thermo Element XR™ ICP-MS at the Plasma Analytical Facility, FSU. Irons were analyzed using a raster scan over a few mm with a 50 µm beam, scanned at 10 µm/s, 50 Hz repetition rate. This technique yielded more representative sampling of the kamacite-taenite banding, but failed to yield useful Ge abundances for Klamath Falls. To obtain more precise Ge, a set of five 150 µm spots were analyzed at 50 Hz for 20 seconds on five of the irons, including both slabs of Klamath Falls. This produced a sufficiently bright beam to resolve Ge. Standardization techniques followed [6].

Results: The IIIFs form distinct siderophile element patterns in Fig. 1, in order of decreasing Os-Ir: Nelson County>Clark County, Oakley, Zinder>St. Genevieve County, Moonbi>> Klamath Falls.

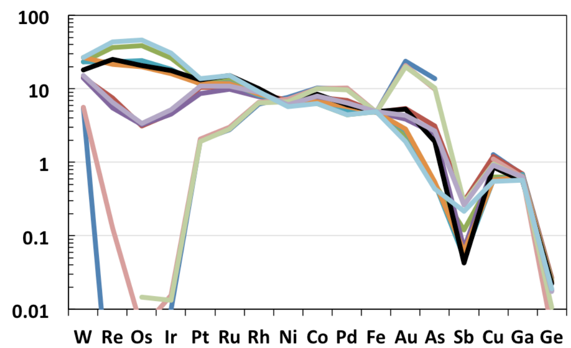

Figure 1: CI-normalized siderophile element abundances for data from this study in order of decreasing condensation temperatures. Zinder is the black line.

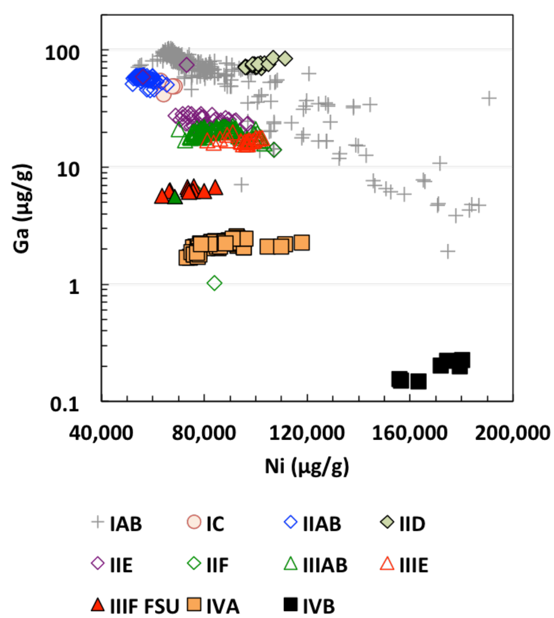

Figure 2. Ga vs. Ni in iron meteorites, showing Zinder (solid green triangle) plotting in the IIIFs (solid red triangles, this study) with other irons from [7-9].

The IIIFs and Zinder share the same Ga, Ge and Sb abundances, although Sb is near the detection limit in IIIFs. Zinder plots on IIIF trends of Co, Ni, As, Ru, Rh, W and Pt vs. Au. In agreement with [10], the range in Ir abundances, from Nelson County to Klamath Falls, was ~2,000, a range exceeded only by IIAB irons [7]. However, in plots of Re, Os and Ir vs. Au, Zinder plots to higher Au at a given Ir abundance (Figure 3).

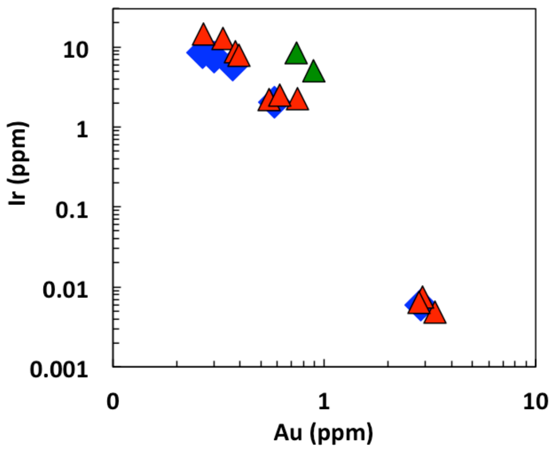

Figure 3. Ir vs. Au trend of IIIFs (UCLA: blue [10]; FSU: red triangles; Zinder: green triangles).

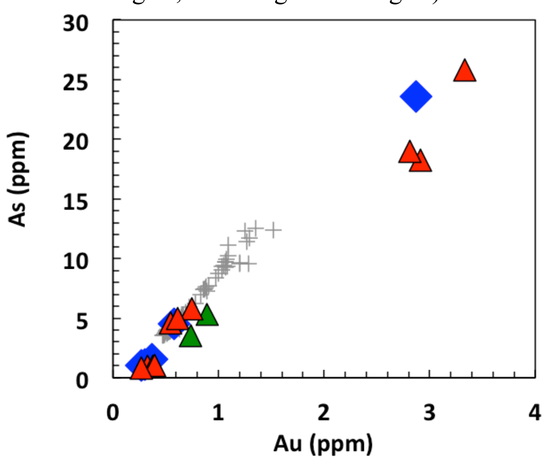

Figure 4. As vs. Au trend of IIIFs (UCLA: blue [8]; FSU: red triangles; Zinder: green triangles) compared with IIABs [7].

A challenge for LA-ICP-MS analyses is representative sampling of the taenite-kamacite lamellae in non-ataxite irons. The partitioning of Au and As between kamacite and taenite is a useful indicator of sampling, since Au and As follow each other closely in magmatic processes, but Au preferentially partitions into taenite while As preferentialy partitions into kamacite. Figure 4 shows that both Zinder analyses oversampled taenite resulting in higher Au.

Discussion:

Relationship between IIIF irons and Zinder metal. The IIIFs were first defined as a new group based on distinct ranges of Ga (6.3-7.2 ppm) and Ge (0.7-1.1 ppm) abundances. Klamath Falls was later recognized as the most evolved member of the IIIF irons [11]. Confirmation of the magmatic nature of IIIFs was provided by [10]. Among IIIFs, this study has not measured Cerro del Inca and Binya, which have intermediate values of Ir. We measured Ga and Ge abundances in Fitzwater Pass consistent with IABs. The metal of Zinder matches the metal of IIIFs closely in Ga and Ge abundances (Fig. 2). The Zinder metal also plots on the magmatic trends of IIIF irons, with the exception of the most compatible elements. As noted above, this is due to oversampling of taenite in Zinder. Chemically, the metal in Zinder is identical to IIIF irons.

Implications for future isotopic studies. The oxygen isotope composition of Zinder plots slightly above the TFL near the eucrites at $\delta^{18}O$= 3.4 ‰, $\Delta^{17}O$= +0.09 ‰ [12]. This composition is near a number of achondrites that are not regarded as genetically related to carbonaceous chondrites based on O, Cr and Ti isotopes, including HEDs, Mars, brachinites, acapulcoites and lodranites [1,2]. Silicates from the Eagle Station pallasites and a number of ungrouped irons (e. g., Mbosi, Tucson, Deep Springs) plot at $\Delta^{17}O$ ~2 permil below this range, near the CAI mixing line [1]. The link between oxygen isotopes and Mo isotopes is still tenous as ureilites, which plot on the CAI mixing line in $\Delta^{17}O$ [1], were shown to be on the NC line in Mo isotopes [13], while Eagle Station Pallasites plot on the CC line in Mo isotopes [3]. Further tests of the relationship between O-Cr-Ti and Mo isotopes are essential for a better understanding of the provenance value of these systems and Zinder affords such an opportunity.

References:

[1] Clayton R. N. and Mayeda T. K. (1996) *GCA 60,* 1999-2017. [2] Warren P. H. (2011) *EPSL 311,* 93-100. [3] Budde G. et al. (2016) *EPSL 454,* 293-303. [4] Kruijer T. S. et al. (2017) *PNAS 114*, 6712-6716. [5] Boesenberg J. S. et al. (2017) *LPSC XLVIII*, Abstract #2319. [6] Humayun M. (2012) *MAPS 47*, 1191-1208. [7] Wasson J. T. et al. (2007) *GCA 71*, 760-781. [8] Scott E. R. D. and Wasson J. T. (1976) *GCA 40*, 103-115. [9] Scott E. R. D. (1978) , GCA 42, 1243-1251. [10] Pernicka E. and Wasson J. T. (1987) *GCA 51*, 1717-1726. [11] Kracher A. et al. (1980) *GCA 44*, 773-787. [12] Bunch T. E. et al. (2005) *MAPS 40*, A26. [13] Budde G. et al. (2017) *80th MetSoc*, Santa Fe, Abstract #6271.